

Energetically Demanding Transport in a Supramolecular Assembly

Chuyang Cheng,[†] Paul R. McGonigal,[†] Wei-Guang Liu,[‡] Hao Li,[†] Nicolaas A. Vermeulen,[†] Chenfeng Ke,[†] Marco Frasconi,[†] Charlotte L. Stern,[†] William A. Goddard III,[‡] and J. Fraser Stoddart^{*,†}

[†]Department of Chemistry, Northwestern University, Evanston, Illinois 60208, United States

[‡]Materials and Process Simulation Center, California Institute of Technology, Pasadena, California 91125, United States

Supporting Information

ABSTRACT: A challenge in contemporary chemistry is the realization of artificial molecular machines that can perform work in solution on their environments. Here, we report on the design and production of a supramolecular flashing energy ratchet capable of processing chemical fuel generated by redox changes to drive a ring in one direction relative to a dumbbell toward an energetically uphill state. The kinetics of the reaction pathway juxtapose a low energy [2]pseudorotaxane that forms under equilibrium conditions with a high energy, metastable [2]-pseudorotaxane which resides away from equilibrium.

The active transport of ions and small molecules across cell membranes, driven by bespoke biochemical machinery, plays a pivotal role in the operation of cells.¹ Nature's transmembrane protein pumps create concentration gradients of ions, such as Na⁺, K⁺ and Ca²⁺, in addition to protons,² whose stored potential may then be used as a secondary energy resource³ in metabolic processes, e.g., ATP synthesis.⁴ During billions of years of evolution, these proteins have developed finely tuned secondary and tertiary structures capable of harnessing external fuel to exert precise control over the noncovalent forces—the potential energy landscape of energy barriers and wells—experienced by their cargos in order to drive them energetically uphill, temporarily away from thermodynamic equilibrium.⁵

Over the past 30 years, chemists have taken advantage of the restricted degrees of freedom available to the components of rotaxanes⁶ and pseudorotaxanes⁷ to construct and control increasingly sophisticated artificial molecular switches that exhibit large amplitude relative motions between their constituent parts.⁸ In the majority of cases, however, the application of a stimulus to these artificial systems induces molecular motions toward a low-energy equilibrium state. The development of artificial molecular assemblies⁹ that can drive a cargo away from its equilibrium position by manipulating kinetic pathways—thereby mimicking the function of their biochemical counterparts—is still very much in its infancy.¹⁰ Here, we report a family of synthetic supramolecular pumps that exploit chemical energy to drive a ring away from its initial state in solution to form metastable, energetically demanding products that can then gradually decay back toward equilibrium. Control of this supramolecular transport is exercised by influencing the kinetics of the reaction pathway using only reversible noncovalent bonding interactions and without the need to make or break

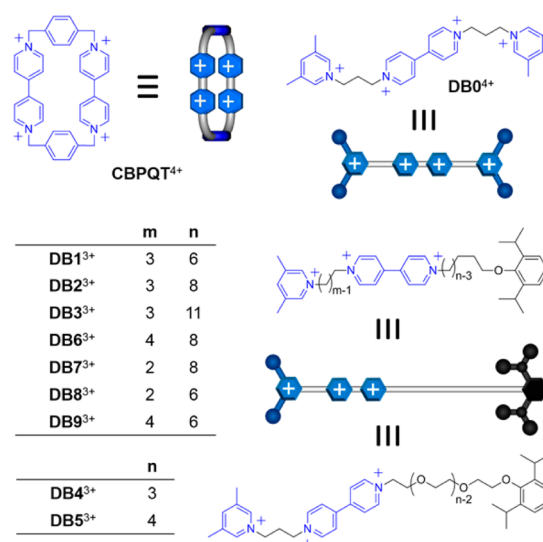


Figure 1. Structural formulas and simplified graphical representations of the CBPQT⁴⁺ ring, the symmetrical dumbbell DBO⁴⁺ and the nine 'one-stroke supramolecular pumps' DB1–9³⁺ employed in this structure–function investigation. Charges are balanced by PF₆[−] counterions which are omitted for the sake of clarity.

covalent bonds. The end result is that the ring is ensnared on an oligomethylene chain¹¹ for which it has little to no binding affinity at any stage of the pumping process.

We designed (Figure 1) a homologous series of dumbbells DB1–9³⁺ bearing 4,4'-bipyridinium (BIPY²⁺) units as radical recognition sites¹² for cyclobis(paraquat-*p*-phenylene)¹³ (CBPQT⁴⁺). A 3,5-dimethylpyridinium (PY⁺) unit is attached to one side of the BIPY²⁺ unit by a short oligomethylene chain, while a bulky stopper is attached to the other side by a longer chain. Before testing the dumbbells, a symmetrical derivative DBO⁴⁺ (Figure 1) was prepared as a model compound to confirm that CBPQT^{2(+•)} can thread across the PY⁺ barrier in order to form the triradical complex DBO^{3+••}•CBPQT^{2(+•)} under the reducing conditions that can bring about radical–radical interactions. The absorption spectra of the radical cation DBO^{3+••} and diradical dication CBPQT^{2(+•)} were first of all recorded separately in MeCN at concentrations of 10^{−4} M. No absorption indicative of BIPY²⁺ dimerization was observed in the near-IR (NIR) region under these conditions. By contrast, when

Received: August 21, 2014

Published: September 25, 2014

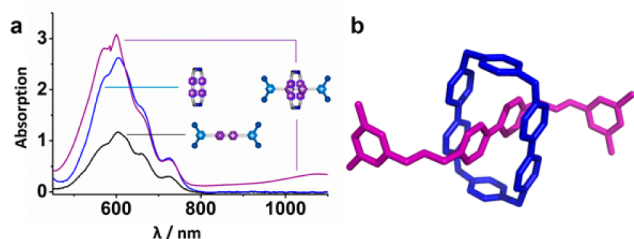


Figure 2. UV-vis-NIR absorption spectroscopic and single crystal XRD evidence that $\text{CBPQT}^{2(+\bullet)}$ threads across the Coulombic PY^+ barrier. (a) Spectra of $\text{DBO}^{3+\bullet}$ (black trace), $\text{CBPQT}^{2(+\bullet)}$ (blue trace), and a 1:1 mixture of $\text{DBO}^{3+\bullet}$ and $\text{CBPQT}^{2(+\bullet)}$ (purple trace). The broad peak around 1100 nm indicates formation of the triradical inclusion complex $\text{DBO}^{3+\bullet}\text{CBPQT}^{2(+\bullet)}$. $[\text{DB}^{4+}] = 1.0 \times 10^{-4} \text{ M}$, $[\text{CBPQT}^{4+}] = 1.0 \times 10^{-4} \text{ M}$. Solvent, MeCN; $T = 298 \text{ K}$. (b) A tubular representation of the solid-state superstructure of $(\text{DBO}0\text{CBPQT}) \cdot 6\text{PF}_6$.^{14,15} Solvent molecules, hydrogen atoms, and counterions are omitted for the sake of clarity.

DBO^{4+} and CBPQT^{4+} were reduced together, a distinctive purple solution was obtained within seconds and UV-vis-NIR spectroscopy revealed (Figure 2a) features characteristic of BIPY^{\bullet} radical-radical interactions, including a broad NIR band around 1100 nm that is indicative¹² of the formation of the triradical inclusion complex $\text{DBO}^{3+\bullet}\text{CBPQT}^{2(+\bullet)}$. Single crystals of $(\text{DBO}0\text{CBPQT}) \cdot 6\text{PF}_6$ suitable for X-ray diffraction (XRD)¹⁴ were grown in a glovebox.¹⁵ The solid-state superstructure confirmed (Figure 2b) that the ring encircles the dumbbell.

With the viability of complex formation between $\text{CBPQT}^{2(+\bullet)}$ and $\text{DBO}^{3+\bullet}$ verified, we hypothesized that subjecting a mixture of CBPQT^{4+} and a dumbbell $\text{DBI}^{\text{9}3+}$ (Figure 1) to a cycle of reduction and oxidation would result in the formation of a high-energy [2]pseudorotaxane. To test our hypothesis, activated zinc dust was added to a 1:1 mixture of DBI^{3+} and CBPQT^{4+} in CD_3CN , giving a purple solution indicative of triradical complex formation within a few seconds. After filtration to remove the excess of zinc, tris(4-bromophenyl)ammonium hexachloroantimonate (magic blue) was added at 0°C to reoxidize the radical species to their fully charged states, and a ^1H NMR spectrum was recorded. Comparison of the ^1H NMR spectra of the dumbbell, the reaction mixture, and the ring revealed (Figure 3a,b,d) formation of a product species in $\sim 80\%$ yield that exhibited broadening ($H_{\alpha/\beta}$) and splitting (H_{CH_2}) of resonances associated with the ring as well as significant upfield shifts of the methylene proton resonances H_{1-4} of the dumbbell component, indicating the formation of $\text{DBI}^{3+}\text{CBPQT}^{4+}$ in which the ring encircles the hexamethylene chain.^{12b,d} This [2]pseudorotaxane was found to be metastable and to dissociate entirely within half an hour at room temperature or within 4 h at 279 K (Figure 3c). Changes in the relative proportions of $\text{DBI}^{3+}\text{CBPQT}^{4+}$ and its separated components were monitored (Figure S4)¹⁵ by ^1H NMR spectroscopy at a constant temperature (279 K) which revealed (Figure 3e) that the dethreading displays first-order kinetics with a rate constant $k = (8.4 \pm 0.6) \times 10^{-5} \text{ s}^{-1}$. Based upon these data, the transition-state energy barrier (ΔG^\ddagger) for the CBPQT^{4+} ring to dissociate from DBI^{3+} by slipping over its positively charged BIPY^{2+} and PY^+ units was found to be $21.5 \text{ kcal mol}^{-1}$.

It appears, therefore, that the design of dumbbell DBI^{4+} allows it to “pump” a ring actively onto its hexamethylene chain following potential energy surfaces resembling those represented as curves in Scheme 1. Initially, the tetracationic CBPQT^{4+} ring is repelled (Scheme 1a) by both the PY^+ and BIPY^{2+} units. Reduction, however, simultaneously lowers the kinetic barrier to threading^{7d} that comes from Coulombic repulsion between the PY^+ unit and the ring, while also bringing radical-radical interactions into play to create (Scheme 1b) a new global minimum in which the dumbbell is encircled by the ring. As a result, the ring slips over the PY^+ unit to form (Scheme 1c) a thermodynamically stable triradical inclusion complex¹² $\text{BIPY}^{\bullet}\text{CBPQT}^{2(+\bullet)}$. A subsequent oxidation step to restore the repulsion between the highly charged ring and dumbbell components^{12d} then imparts a driving force for the CBPQT^{4+} ring to undergo translational motion. In thermodynamic terms, the global energy minimum would be reached if the ring were to

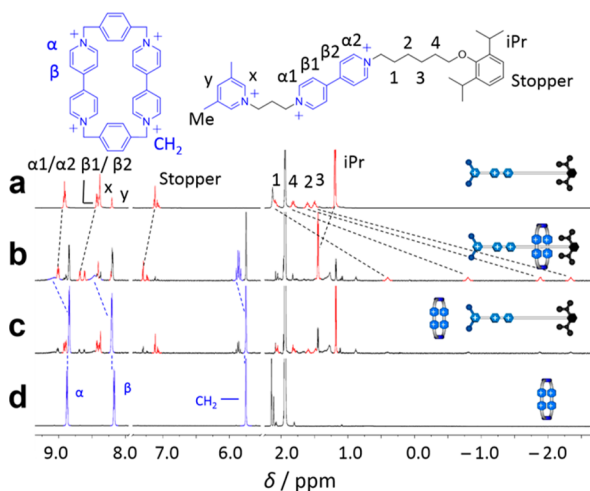
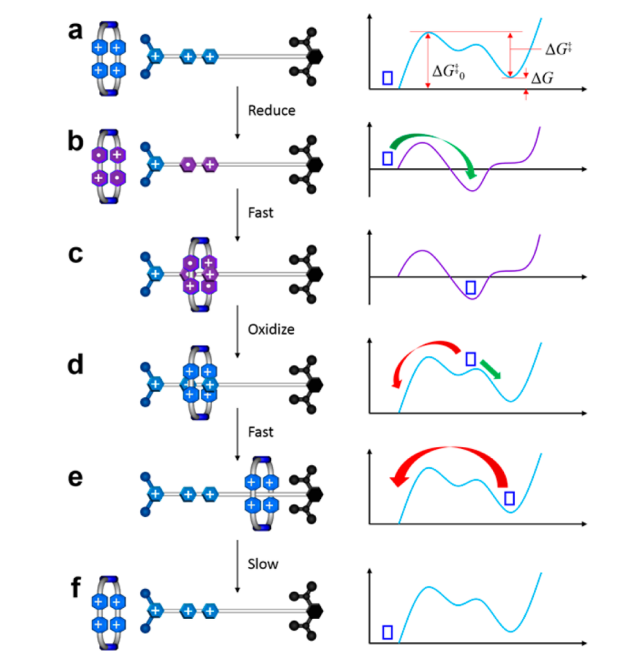


Figure 3. ^1H NMR spectroscopic analysis of [2]pseudorotaxane formation and the kinetic barrier to dissociation. Partial ^1H NMR spectra (600 MHz, CD_3CN , 279 K) of (a) the dumbbell DBI^{3+} , (b) a reaction mixture containing $\text{DBI}^{3+}\text{CBPQT}^{4+}$ after performing a cycle of reduction and oxidation, (c) after standing at 279 K for 4 h, and (d) CBPQT^{4+} . Peaks are highlighted in red and blue for DBI^{3+} and CBPQT^{4+} , respectively. The changes in chemical shifts (blue and black dashed lines) are indicative of [2]pseudorotaxane formation. (e) Plot of the change in molar fraction over time at 279 K based on integration of the ^1H NMR spectra. Inset: linear relationship between $-\ln(c/c_0)$ and time, indicating that the dethreading process obeys first-order kinetics. The activation barrier ΔG^\ddagger was calculated using the Eyring equation.

Scheme 1. Graphical Representation of the Pumping Mechanism and Corresponding Energy Profiles



retrace its path and dissociate from the dumbbell. The electrostatic barrier to translation originating from the PY^+ group, however, is restored upon oxidation, kinetically disfavoring the backward pathway and forcing the ring to shuttle away (Scheme 1d) in the opposite direction. Consequently, the CBPQT^{4+} ring is ensnared (Scheme 1e) as part of a metastable [2]pseudorotaxane that does not benefit from stabilizing noncovalent bonding interactions. Indeed, the enforced proximity of the three charged viologen units dictates that the [2]pseudorotaxane resides in an energetically demanding state compared to its separated components.

By performing the same reduction and oxidation protocol with the entire homologous series of dumbbells DB2-8^{3+} , we were able to gain some insight into the relationship between the structure and energetics of the supramolecular pumps. Extension of the oligomethylene chain between the BIPY^{2+} and stopper units resulted in two pseudorotaxanes, namely $\text{DB2}^{3+}\text{CBPQT}^{4+}$ and $\text{DB3}^{3+}\text{CBPQT}^{4+}$, that exhibited prolonged half-lives compared to $\text{DB1}^{3+}\text{CBPQT}^{4+}$. The dissociations of $\text{DB2}^{3+}\text{CBPQT}^{4+}$ and $\text{DB3}^{3+}\text{CBPQT}^{4+}$ were monitored by ^1H NMR spectroscopy at 331 and 365 K, respectively, which allowed the kinetic barriers to dethreading to be determined (Figures S5 and S6)¹⁵ as 25.3 and 29.0 kcal mol⁻¹. Although the intrinsic barrier to association ΔG^\ddagger_0 (Scheme 1a), which stems mainly from Coulombic repulsion between positively charged $\text{BIPY}^{2+}/\text{PY}^+$ units and the CBPQT^{4+} ring, is similar for dumbbells DB1-3^{3+} , the large variation in the kinetic barriers to dethreading can be rationalized by considering the difference in the Gibbs free energy ΔG of the metastable [2]pseudorotaxanes. A shorter oligomethylene chain confines the like-charged CBPQT^{4+} ring and BIPY^{2+} unit in closer proximity to one another, destabilizing the pseudorotaxane and resulting in a higher ΔG .^{12d} Density functional theory (DFT) calculations support this reasoning. We calculated (Table S3)¹⁵ increases in enthalpy (ΔH) of 14.9, 8.8, and 7.0 kcal mol⁻¹ for the [2]pseudorotaxanes based on DB1^{3+} , DB2^{3+} , and DB3^{3+} , respectively, compared to their separated components.

The oligomethylene portion of the dumbbell can be replaced by an oligoethylene glycol chain without diminishing the efficiency of the pumping process. Dumbbells DB4^{3+} and DB5^{3+} , bearing triethylene glycol and tetraethylene glycol tails, respectively, gave rise to [2]pseudorotaxanes in ~85% yield, as estimated by ^1H NMR spectroscopy.¹⁵ While the dissociation of $\text{DB4}^{3+}\text{CBPQT}^{4+}$ follows (Figure S7)¹⁵ first-order kinetics in a manner consistent with the oligomethylene derivatives, our observations indicate that the dissociation (Figure S8)¹⁵ of $\text{DB5}^{3+}\text{CBPQT}^{4+}$ is autocatalytic. The most probable explanation for this phenomenon is that hydrogen bonding between the tetraethylene glycol chain and CBPQT^{4+} ring, which is a well-established interaction,¹⁶ stabilizes the transition state to dethreading.^{7d,17} Indeed, the addition of 1.0 equiv of dumbbell DB5^{3+} to a solution of $\text{DB5}^{3+}\text{CBPQT}^{4+}$ accelerated the dissociation of the [2]pseudorotaxane.¹⁵ In order to avoid this complication in subsequent investigations, we decided to limit dumbbell design to those containing oligomethylene chains.

Having explored the effect of altering the length and nature of the chain between the BIPY^{2+} unit and the stopper, we turned our attention to assessing the influence of the short oligomethylene linker connecting the Coulombic barrier PY^+ to the rest of the dumbbell. Taking DB2^{3+} as a point of reference, two dumbbells were synthesized bearing a butylene (DB6^{3+}) and a bismethylene (DB7^{3+}) linker in place of the propylene one in DB2^{3+} . Surprisingly, this seemingly minor alteration in molecular structure was found to have a dramatic effect on the outcomes of redox cycling. Subjecting a mixture of CBPQT^{4+} and DB6^{3+} to the standard protocol gave only a physical mixture after reduction and oxidation (Figure S9),¹⁵ suggesting that elongating the linker diminishes considerably the ability of the BIPY^{2+} and PY^+ units to act together in creating a highly charged end group that retains the ring on the dumbbell on account of Coulombic repulsion. In contrast, when CBPQT^{4+} and DB7^{3+} were reduced and oxidized under the same conditions, a bench stable [2]rotaxane was produced that could be isolated (Figure S1)¹⁵ and fully characterized by NMR spectroscopy and mass spectrometry. Indeed, the stability of the mechanically interlocked product precluded measurement of any barrier to dethreading; no dissociation could be observed (Figure S10),¹⁵ even after refluxing in MeCN for 18 h! In order to quantify the change in the energy barrier that occurs upon shortening the propylene linker, we prepared DB8^{3+} with a bismethylene linker and a hexamethylene chain on which to collect the ring, rather than the octamethylene one in DB7^{3+} . The [2]pseudorotaxane $\text{DB8}^{3+}\text{CBPQT}^{4+}$ dissociates at 355 K with a rate constant $k = (2.2 \pm 0.1) \times 10^{-5} \text{ s}^{-1}$, corresponding to a dethreading barrier of 28.5 kcal mol⁻¹ (Figure S11).¹⁵ It is quite remarkable that, with the removal of a single methylene group from DB1^{3+} (propylene linker) to give DB8^{3+} (bismethylene linker), we observe an increase of 7.0 kcal mol⁻¹ in the barrier to dissociation, from 21.5 to 28.5 kcal mol⁻¹. This phenomenon can be accounted for to a certain extent by considering that the magnitude of Coulombic forces are inversely proportional to the square of the distance between two charged species and that the longer the linker, the further the ring resides away from the PY^+ unit. DFT calculations indicate, however, that the interplay between the PY^+ and BIPY^{2+} units also plays a role. The calculated potential energy profile for dissociation of $\text{DB8}^{3+}\text{CBPQT}^{4+}$ is characterized (Figure S12)¹⁵ by one major energy barrier of 18.7 kcal mol⁻¹. The profile of a model [2]pseudorotaxane analog that contains a butylene linker, $\text{DB9}^{3+}\text{CBPQT}^{4+}$, exhibits (Figure S13)¹⁵ two smaller barriers, the highest of which is only 12.4 kcal/mol. It

appears, therefore, that the dense buildup of charge between closely tethered BIPY²⁺ and PY⁺ units (e.g., in DB7–8³⁺) acts in an additive manner in repelling the slippage of the CBPQT⁴⁺ ring, although this effect is diminished if a longer spacer is employed.¹⁹

In summary, we have designed, synthesized, and operated a family of artificial supramolecular pumps which couple the dissipation of redox chemical energy to the formation of a non-equilibrium state. The alternation between the asymmetric potential energy surfaces that they create shapes the kinetically favored pathway followed by a positively charged ring, leading to a metastable [2]pseudorotaxane in which the ring is trapped on a dumbbell in the absence of any stabilizing interactions. By studying a homologous series of supramolecular pumps and their respective [2]pseudorotaxanes, we have elucidated the delicate balance between molecular structure and the energetics of the pumping process. Judicious choice of molecular structure allows for both high-efficiency [2]pseudorotaxane formation and the regulation of its subsequent dissociation over a Coloumbic barrier, which can be tuned within a range >10 kcal mol⁻¹. The supramolecular pumps we have described exhibit some of the qualities of the active transport^{1,2} of ions and small molecules that takes place in Nature—i.e., they harness an energy input in order to oscillate between asymmetric potential energy surfaces and, thus, transport a species to a high-energy state. In their current form, however, these synthetic supramolecular pumps are unable to act in the repetitive manner reminiscent of their natural counterparts in order to push a system incrementally further and further from equilibrium, as occurs, e.g., when carrier proteins create concentration gradients. By bringing the knowledge gained in this structure–function study to bear on the design of synthetic supramolecular pumps, it may be possible to devise more sophisticated systems capable of this kind of repetitive and progressive action.

■ ASSOCIATED CONTENT

📄 Supporting Information

Detailed synthesis procedures and characterization data (NMR spectroscopy and mass spectrometry) for all compounds. UV–vis–NIR spectroscopic and single crystal XRD characterization of the [2]pseudorotaxane (DB0CCBPQT)·6PF₆. This material is available free of charge via the Internet at <http://pubs.acs.org>.

■ AUTHOR INFORMATION

Corresponding Author

stoddart@northwestern.edu

Notes

The authors declare no competing financial interest.

■ ACKNOWLEDGMENTS

This material is based on work supported by the National Science Foundation (NSF) under CHE-1308107. W.-G.L. and W.A.G. thank NSF (CMMI-1120890 and EFRI-1332411) for financial support and to ONR-DURIP and NSF-CSEM for computing resources.

■ REFERENCES

(1) Higgins, C. F. *Annu. Rev. Cell. Biol.* **1992**, *8*, 67.
 (2) (a) Skou, J. C. *Angew. Chem., Int. Ed.* **1998**, *37*, 2321. (b) Kaplan, J. H. *Annu. Rev. Biochem.* **2002**, *71*, 511. (c) MacLennan, D. H.; Rice, W. J.; Green, N. M. *J. Biol. Chem.* **1997**, *272*, 28815. (d) Lozier, R. H.; Bogomolni, R. A.; Stoerkenius, W. *Biophys. J.* **1975**, *15*, 955.

(3) (a) Wright, E. M.; Loo, D. D. F.; Hirayama, B. A. *Physiol. Rev.* **2011**, *91*, 733. (b) West, I. C. *Biochim. Biophys. Acta* **1980**, *604*, 91.

(4) (a) Walker, J. E. *Angew. Chem., Int. Ed.* **1998**, *37*, 2309. (b) Elston, T.; Wang, H. Y.; Oster, G. *Nature* **1998**, *391*, 510. (c) Boyer, P. D. *Angew. Chem., Int. Ed.* **1998**, *37*, 2297.

(5) (a) Gai, F.; Hasson, K. C.; McDonald, J. C.; Anfinrud, P. A. *Science* **1998**, *279*, 1886. (b) Subramaniam, S.; Henderson, R. *Nature* **2000**, *406*, 653. (c) Astumian, R. D. *Nat. Nanotechnol.* **2012**, *7*, 684.

(6) Stoddart, J. F. *Chem. Soc. Rev.* **2009**, *38*, 1802.

(7) (a) Nygaard, S.; Laursen, B. W.; Flood, A. H.; Hansen, C. N.; Jeppesen, J. O.; Stoddart, J. F. *Chem. Commun.* **2006**, 144. (b) Arduini, A.; Bussolati, R.; Credi, A.; Monaco, S.; Secchi, A.; Silvi, S.; Venturi, M. *Chem.-Eur. J.* **2012**, *18*, 16203. (c) Baroncini, M.; Silvi, S.; Venturi, M.; Credi, A. *Angew. Chem., Int. Ed.* **2012**, *51*, 4223. (d) Li, H.; Cheng, C. Y.; McGonigal, P. R.; Fahrenbach, A. C.; Frascioni, M.; Liu, W. G.; Zhu, Z. X.; Zhao, Y. L.; Ke, C. F.; Lei, J. Y.; Young, R. M.; Dyar, S. M.; Co, D. T.; Yang, Y. W.; Botros, Y. Y.; Goddard, W. A., III; Wasielewski, M. R.; Astumian, R. D.; Stoddart, J. F. *J. Am. Chem. Soc.* **2013**, *135*, 18609.

(8) (a) Balzani, V.; Credi, A.; Raymo, F. M.; Stoddart, J. F. *Angew. Chem., Int. Ed.* **2000**, *39*, 3349. (b) Collin, J.-P.; Heitz, V.; Sauvage, J.-P. *Top. Curr. Chem.* **2005**, *262*, 29.

(9) (a) Feringa, B. L. *J. Org. Chem.* **2007**, *72*, 6635. (b) Michl, J.; Sykes, E. C. H. *ACS Nano* **2009**, *3*, 1042. (c) Vogelsberg, C. S.; Garcia-Garibay, M. A. *Chem. Soc. Rev.* **2012**, *41*, 1892.

(10) (a) Serreli, V.; Lee, C. F.; Kay, E. R.; Leigh, D. A. *Nature* **2007**, *445*, 523. (b) Kay, E. R.; Leigh, D. A.; Zerbetto, F. *Angew. Chem., Int. Ed.* **2007**, *46*, 72. (c) Coskun, A.; Banaszak, M.; Astumian, R. D.; Stoddart, J. F.; Grzybowski, B. A. *Chem. Soc. Rev.* **2012**, *41*, 19.

(11) (a) Goldup, S. M.; Leigh, D. A.; McBurney, R. T.; McGonigal, P. R.; Plant, A. *Chem. Sci.* **2010**, *1*, 383. (b) Sevick, E. M.; Williams, D. R. M. *Molecules* **2013**, *18*, 13398.

(12) (a) Trabolsi, A.; Khashab, N.; Fahrenbach, A. C.; Friedman, D. C.; Colvin, M. T.; Coti, K. K.; Benítez, D.; Tkatchouk, E.; Olsen, J. C.; Belowich, M. E.; Carmielli, R.; Khatib, H. A.; Goddard, W. A., III; Wasielewski, M. R.; Stoddart, J. F. *Nat. Chem.* **2010**, *2*, 42. (b) Li, H.; Fahrenbach, A. C.; Dey, S. K.; Basu, S.; Trabolsi, A.; Zhu, Z. X.; Botros, Y. Y.; Stoddart, J. F. *Angew. Chem., Int. Ed.* **2010**, *49*, 8260. (c) Fahrenbach, A. C.; Barnes, J. C.; Lanfranchi, D. A.; Li, H.; Coskun, A.; Gassensmith, J. J.; Liu, Z. C.; Benítez, D.; Trabolsi, A.; Goddard, W. A., III; Elhabiri, M.; Stoddart, J. F. *J. Am. Chem. Soc.* **2012**, *134*, 3061. (d) Li, H.; Zhu, Z. X.; Fahrenbach, A. C.; Savoie, B. M.; Ke, C. F.; Barnes, J. C.; Lei, J. Y.; Zhao, Y. L.; Lilley, L. M.; Marks, T. J.; Ratner, M. A.; Stoddart, J. F. *J. Am. Chem. Soc.* **2013**, *135*, 456.

(13) Odell, B.; Reddington, M. V.; Slawin, A. M. Z.; Spencer, N.; Stoddart, J. F.; Williams, D. J. *Angew. Chem., Int. Ed.* **1988**, *27*, 1547.

(14) Crystals were grown by slow vapor diffusion of iPr₂O into a MeCN solution at 0 °C. Crystal data for C₈₂H₉₄F₃₆N₁₆P₆ (M = 2173.55): monoclinic, space group P21/c (no. 14), a = 18.8758(10), b = 20.3394(13), c = 13.1067(8) Å, β = 104.883(3)°, V = 4863.1(5) Å³, T = 99.98 K, Z = 2, μ(CuKα) = 2.114, 30255 reflections measured, 8210 unique (R_{int} = 0.0327) which were used in all calculations. wR(F₂) = 0.1898. CCDC 1019889.

(15) See the SI.

(16) Zhu, Z. X.; Li, H.; Liu, Z. C.; Lei, J. Y.; Zhang, H. C.; Botros, Y. Y.; Stern, C. L.; Sarjeant, A. A.; Stoddart, J. F.; Colquhoun, H. M. *Angew. Chem., Int. Ed.* **2012**, *51*, 7231.

(17) Andersen, S. S.; Share, A. I.; Poulsen, B. L.; Korner, M.; Duedal, T.; Benson, C. R.; Hansen, S. W.; Jeppesen, J. O.; Flood, A. H. *J. Am. Chem. Soc.* **2014**, *136*, 6373.

(18) (a) Li, H.; Zhao, Y. L.; Fahrenbach, A. C.; Kim, S. Y.; Paxton, W. F.; Stoddart, J. F. *Org. Biomol. Chem.* **2011**, *9*, 2240. (b) Hmadeh, M.; Fahrenbach, A. C.; Basu, S.; Trabolsi, A.; Benítez, D.; Li, H.; Albrecht-Gary, A. M.; Elhabiri, M.; Stoddart, J. F. *Chem.–Eur. J.* **2011**, *17*, 6076.

(19) Taking all of the calculated and experimentally measured thermodynamic data together (Table S18), the fraction of the redox energy input that is stored in the high-energy pseudorotaxanes can be calculated to be between 5 and 10%.